JACS
JOURNAL OF THE AMERICAN CHEMICAL SOCIETY
Article
pubs.acs.org/JACS

Very Rapid DNA-Templated Reaction for Efficient Signal Amplification and Its Steady-State Kinetic Analysis of the Turnover Cycle

Aya Shibata,[†] Takanori Uzawa,[†,⊥] Yuko Nakashima,[†] Mika Ito,[†,‡] Yukiko Nakano,[†] Satoshi Shuto,[‡] Yoshihiro Ito,*[,†,⊥] and Hiroshi Abe*[,†,§,‡,⊥]

[†]Nano Medical Engineering Laboratory, RIKEN Advanced Science Institute, 2-1, Hirosawa, Wako-Shi, Saitama 351-0198, Japan

[‡]Faculty of Pharmaceutical Sciences, Hokkaido University, Kita-12, Nishi-6, Kita-ku, Sapporo 060-0812, Japan

[§]PRESTO, Japan Science and Technology Agency, 4-1-8, Honcho, Kawaguchi, Saitama 332-0012, Japan

[⊥]Emergent Bioengineering Materials Research Team, RIKEN Center for Emergent Matter Science, 2-1, Hirosawa, Wako-Shi, Saitama 351-0198, Japan

Supporting Information

ABSTRACT: Oligonucleotide-templated reactions are powerful tools for the detection of nucleic acid sequences. One of the major scientific challenges associated with this technique is the rational design of non-enzyme-mediated catalytic templated reactions capable of multiple turnovers that provide high levels of signal amplification. Herein, we report the development of a nucleophilic aromatic substitution reaction-triggered fluorescent probe. The probe underwent a rapid templated reaction without any of the undesired background reactions. The fluorogenic reaction conducted in the presence of a template provided a 223-fold increase in fluorescence after 30 s compared with the nontemplated reaction. The probe provided an efficient level of signal amplification that ultimately enabled particularly sensitive levels of detection. Assuming a simple model for the templated reactions, it was possible to estimate the rate constants of the chemical reaction in the presence and in the absence of the template. From these kinetic analyses, it was possible to confirm that an efficient turnover cycle had been achieved, on the basis of the dramatic enhancement in the rate of the chemical reaction considered to be the rate-determining step. With maximized turnover efficiency, it was demonstrated that the probe could offer a high turnover number of 1500 times to enable sensitive levels of detection with a detection limit of 0.5 pM in the catalytic templated reactions.

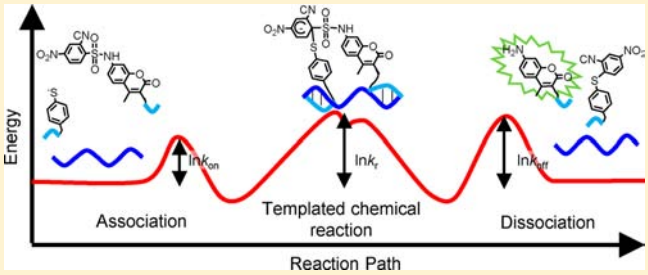

INTRODUCTION

Oligonucleotide-templated reactions have received considerable levels of attention as a potential approach for nucleic acid sensing, with applications including the detection of RNA in living cells.[1] This strategy exploits the target strand as a template for two functionalized probes. For example, native chemical ligation,[2] hydrolysis,[3] the Staudinger reaction,[1c,d,4] transfer of a reporter group,[5] DNAzyme,[6] S_N2 quencher displacement ligation reactions (QUAL probe),[1a,b,7] metal-activated reactions,[8] photocaged reactions,[9] photocatalyst reactions,[10] and metal catalysts[11] have all been applied to the development of fluorescent nucleic acid reactions. These oligonucleotide-templated reactions can provide signal amplification through multiple turnover reactions,[12] and it is generally envisaged that this will enable particularly sensitive levels of detection. Oligonucleotide-templated reactions using a target oligonucleotide as a catalyst (OTRC) provide a simple molecular mechanism for multiple turnover reactions. Furthermore, this strategy only requires two probe pairs and does not require extra reagents to catalyze the reaction or the application of continuous external stimuli to provide a photosensitization step for the signal amplification process. We believe that the rational design of such molecular mechanisms represents an important scientific challenge.

Of the variety of different OTRC chemistries currently available, ligation reactions in particular suffer from several limitations, including the increased affinity of the product for the target oligonucleotide. Under thermodynamic control conditions, inhibition from the product prevents the realization of a high catalytic turnover reaction on the target oligonucleotide. Unligated chemistries have therefore been reported to suppress such product inhibition. In this case, the affinity of the product for the target oligonucleotide remains unchanged after the reaction, and the unreacted probe can therefore be readily replaced by the product on an oligonucleotide target under thermodynamic control. Grossman et al.[5a] reported the achievement of a particularly good result from this approach

Received: May 16, 2013
Published: September 9, 2013

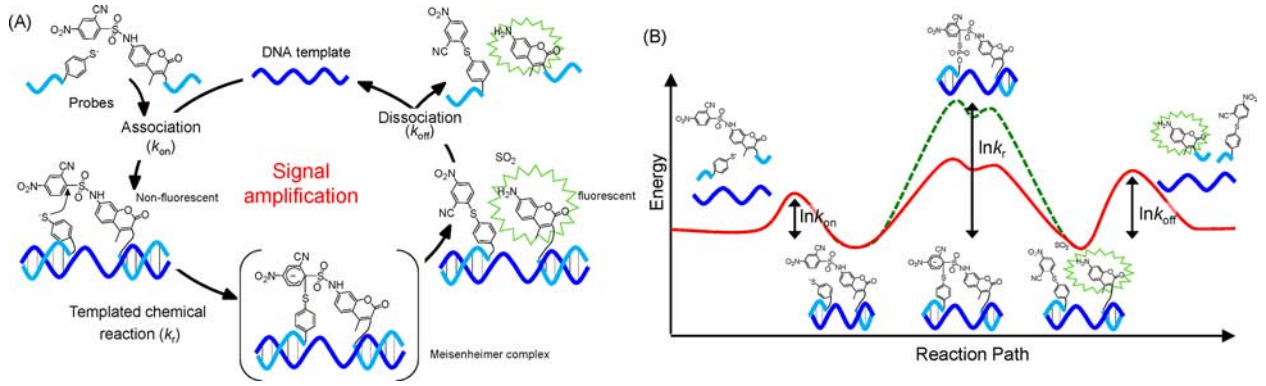

Figure 1. Fluorescence emission of DNs or CNs protected coumarin by nucleophilic substitution reaction. (A) Turnover cycle, (B) Energy diagram of the templated reaction.

for an OTRC where the turnover number reached 402 within 24 h when a 10^4-fold excess of the probes was used for the quencher transfer reaction.

The catalytic turnover cycle for an OTRC is composed of three steps (Figure 1), including (1) the association of the probes to the template; (2) the templated chemical reaction accompanied by a fluorescence signal; and (3) the dissociation of the fluorescent product from the template. To design an efficient signal amplification system, it would be necessary to accelerate the reaction cycle under kinetic control by enhancing the rate of the rate-determining step of the OTRC. To achieve this goal, it would also be necessary to determine which of the three steps of the OTRC that the rate-determining step is. For example, the association or dissociation constants of the short DNA fragment are reported to be 2.0×10^7 M^{-1} s^{-1} and 0.2 s^{-1}, respectively.[13] Staudinger, hydrolysis, and transfer reactions typically exhibit rate constants in the range of 8.32×10^{-8} (ref 5a) to 7.5×10^{-3} s^{-1} (ref 4a). Thus, the chemical reaction providing the rate-determining step in the OTRC cycle is represented by the highest activation barrier in the reaction diagram (Figure 1B). Any acceleration in the rate of the rate-determining chemical reaction should therefore provide an increase in the overall efficiency of the turnover cycle over a certain time period.

An ideal probe for an OTRC would effectively facilitate a high speed templated reaction, a low level of background intermolecular reactions without template assistance together with highly efficient fluorogenic properties. We recently reported the development of a fluorogenic system for a nucleophilic aromatic substitution (S_NAr) reaction-triggered fluorescence probe bearing a 2,4-dinitrobenzenesulfonyl (DNs)-protected aminocoumarin (DNs-AMCA) as the fluorogenic molecule and phosphorothioate (PS) as nucleophilic molecule for an oligonucleotide-templated reaction.[14] Although the fluorogenic system offered a high signal/background (S/B) ratio, the rate of the reaction was slow and did not sufficiently accelerate the turnover cycle. Herein, we report the development of a new ultrarapid fluorogenic-reaction for an OTRC based on a S_NAr reaction between 2-cyano-4-nitrobenzenesulfonyl (CNs)-protected aminocoumarin (CNs-AMCA) as a prefluorophore molecule and 4-mercaptobenzoic acid (MBA) as a nucleophilic molecule. The fluorogenic S_NAr reaction of this new probe occurs rapidly and is 668 times faster than our previously reported DNs-AMCA/PS pair, which was comparable in speed to dissociation step. Furthermore, this new reaction yields a significant fluorescent signal as well as suppressing the undesired background signal, and consequently enables sensitive levels of detection with maximized signal amplification. We also demonstrated that the probe could offer 1500 turnovers. Therefore, to the best of our knowledge, the current system represents the best result ever reported to date for an OTRC.

RESULTS

Design and Synthesis of the Probes. We have previously reported the use of DNs-AMCA and PS as fluorogenic and nucleophilic molecules, respectively, for an oligonucleotide-templated reaction.[14] The rate of the chemical reaction in that particular case, however, was too slow for effective application. To accelerate the rate of this reaction, the use of an MBA group as the nucleophilic molecule was evaluated, because thiophenols are generally expected to be more nucleophilic than PS as a consequence of reduced steric hindrance around the nucleophilic center. We designed a novel CNs-AMCA as the prefluorophore molecule with the expectation that this would exhibit a slightly lower level of reactivity than DNs-AMCA. It was envisaged that this approach would offer a high S/B ratio for the appropriate level of reactivity. The syntheses of the CNs-AMCA and MBA-NHS are shown in Scheme S1 (Supporting Information). The treatment of the AMCA methyl ester **1** with 2-cyano-4-nitrobenzenesulfonyl chloride[15] in a mixture of pyridine/CH_2Cl_2 gave the corresponding CNs-protected material **2** in a 51% yield. Subsequent hydrolysis of **2** with lithium hydroxide afforded CNs-AMCA **3** in a 95% yield. In a separate scheme, the treatment of MBA with *N*-hydroxysuccinimide in DMF for 16 h afforded MBA-NHS **4** in a 19% yield. The fluorogenic DNA probe was synthesized via modification at the 5′ terminal with the DNs- or CNs-AMCA, where the *N*-hydroxysuccinimide ester of the DNs- or CNs-AMCA was reacted with the amino group at the 5′ terminal of the DNA probe (Scheme S2, Supporting Information). The PS and the MBA probes were synthesized via the modification of the 3′ terminal with a phosphorothioate group or the MBA group. The template originating from the 23S rRNA gene sequence in the *Escherichia coli* (*E. coli*) K12 strain was designed in this way.[16]

Reaction of the Fluorogenic Probes with Nucleophilic Molecules. To compare the reactivities of different nucleophilic molecules, thymidine 3′-*O*-(12-(phosphoryloxy) dodecyl *O*,*S*-dihydrogenphosphorothioate) (PS dT) and MBA were tested for their S_NAr reactions using the DNs- and CNs-AMCA probes as the substrates. The pK_a values of these nucleophilic

dx.doi.org/10.1021/ja404743m | J. Am. Chem. Soc. 2013, 135, 14172−14178

groups are 5.3 (PS dT)[17] and 6.0 (MBA),[18] respectively. These nucleophilic groups would therefore exist as the corresponding thioxide anions under neutral conditions at pH 7.2, and should consequently be nucleophilic enough to accelerate the S_NAr reactions with caged AMCA derivatives. The uncaging reaction was evaluated by observing the increase in the intensity of fluorescence signal associated with this transformation. The apparent first-order rate constant, k_{app}, was consequently obtained from the gradient of the plot describing the treatment of the caged AMCA probe with an excess of the nucleophilic molecule (Figure 2, Figure S1, Supporting Information). The

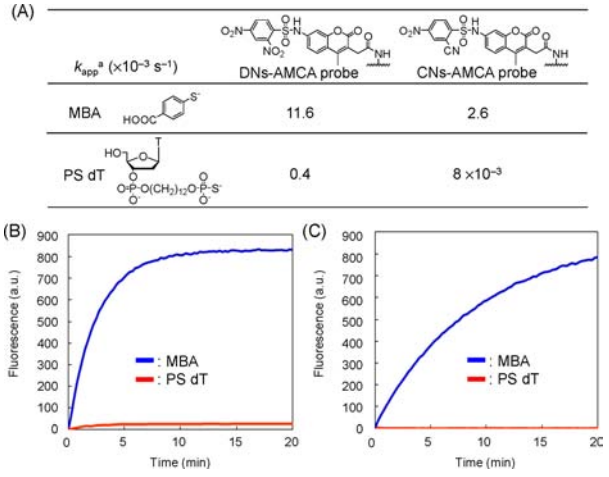

Figure 2. (A) The first-order rate constant of DNs- or CNs-AMCA probe with nucleophilic molecule. (B), (C) Time course of the fluorescence intensity (B: DNs-AMCA probe, C: CNs-AMCA probe). All measurements were done in 20 mM Tris-HCl buffer (pH 7.2) containing 500 nM R-AMCA probe, 500 μM nucleophilic molecule and 100 mM $MgCl_2$ at 22 °C. Reaction was monitored by excitation at 345 nm and emission at 450 nm. [a]Analyzed by linear regression as simple first-order kinetics by Microsoft Excel.

DNs- and CNs-AMCA probes reacted rapidly with MBA to provide a fluorescence signal from the free AMCA, although the rate of the reaction of the DNs-AMCA probe (k_{app} 11.6 × 10^{-3} s^{-1}) was greater than that of the CNs-AMCA probe (k_{app} 2.6 × 10^{-3} s^{-1}).

In contrast, the PS dT reacted at a much slower rate with both of the caged probes, with the corresponding k_{app} values determined to be 4 × 10^{-4} or 8 × 10^{-6} s^{-1}, respectively. MBA drastically increased the rate of the reactions with the DNs-AMCA and CNs-AMCA probes, with the rates increasing 29- and 325-fold, respectively, in comparison with PS dT.

A density functional theory (DFT) calculation was conducted to develop a greater understanding of the reasons behind the observed increases in the rates of the reactions using a series of model compounds (Figure S2, Supporting Information). The activation energies ($\Delta G^{\ddagger}$) of the transition states associated with a series of S_NAr reactions, including CNFB (a model of CNs-AMCA), thiophenol (a model of MBA), and phosphorothioate (model of PS), were calculated at B3LYP/6-31G*. The results revealed that the $\Delta G^{\ddagger}_1$ (CNFB and thiophenol) and $\Delta G^{\ddagger}_2$ (CNFB and phosphorothioate) values were 9.2 and 11.5 kcal/mol, respectively. The rate enhancement between the thiophenol and phosphorothioate was calculated to be 48-fold using the Eyring equation. Theoretical calculations also supported that thiophenol was more nucleophilic than phosphorothioate.

Rapid DNA Templated S_NAr reactions. A systematic study of the S_NAr reaction was conducted by changing the probe pairing between the electrophilic probe (DNs-AMCA or CNs-AMCA) and the nucleophilic probe (PS or MBA) to determine the best partnership of probes that would offer the most rapid templated reaction together with the lowest level of background reactions.

The electrophilic and nucleophilic probes were incubated both in the presence and in the absence of the template under equimolar conditions (500 nM). The fluorescence signals at an emission wavelength of 450 nm were monitored in a time-dependent manner over 60 s, and the conversion yields were calculated on the basis of a comparison with an authentic sample (Figure 3). For the DNs-AMCA probe, the MBA probe

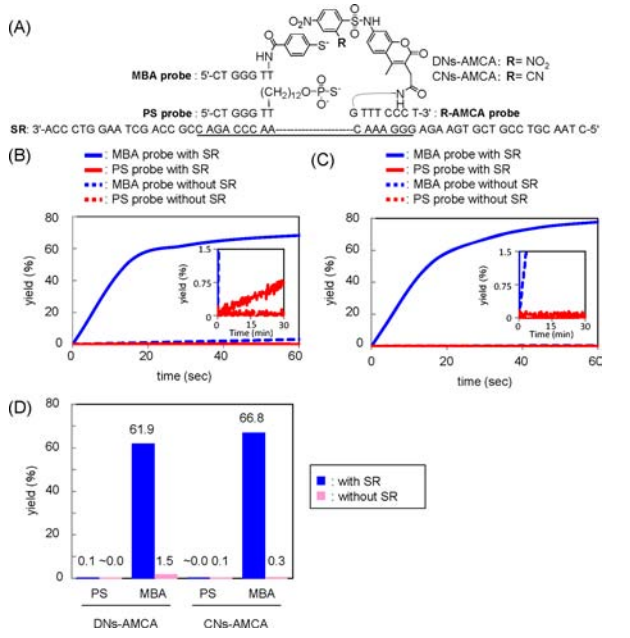

Figure 3. (A) Sequences of oligonucleotides used in this study. The DNs- or CNs-AMCA probe was an 8 mer ODN modified with DNs- or CNs-AMCA at the 5′ terminal. The nucleophilic probe was a 7 mer ODN modified with MBA or phosphorothioate at the 3′ terminal. The DNA targets were 52 mer ODNs (SR). The target sequence is underlined. (B), (C) Time course of the yield in the reaction between 500 nM MBA or PS probe and 500 nM R-AMCA probe (B: DNs-AMCA, C: CNs-AMCA) with or without 500 nM SR in 20 mM Tris-HCl buffer (pH 7.2) containing 100 mM $MgCl_2$ at 22 °C. Reaction was monitored by excitation at 345 nm and emission at 450 nm. (D) The yield of templated reaction after 30 s.

showed a surprisingly rapid rate of reaction, with the reaction progressing to 60% conversion after 20 s and reaching the saturation phase (Figure 3B). The inflection point of the DNs-AMCA probe was determined to be 37.8 s. In contrast, the rate of the reaction with the PS probe was much slower, with the reaction only progressing to 1% conversion after 30 min. One of the major limitations associated with the use of the DNs-AMCA/MBA probe pair, however, was the occurrence of a slight background reaction in the absence of the template (Figure 3B, Figure S3, Supporting Information). The S/B ratio was calculated to be 41 after 30 s (Figure 3D).

We then proceeded to evaluate the reaction of the CNs-AMCA probe with the MBA probe (Figure 3C). Once again, the MBA probe provided a rapid rate of reaction that was similar to the rate observed from its combination with DNs-

dx.doi.org/10.1021/ja404743m | J. Am. Chem. Soc. 2013, 135, 14172−14178

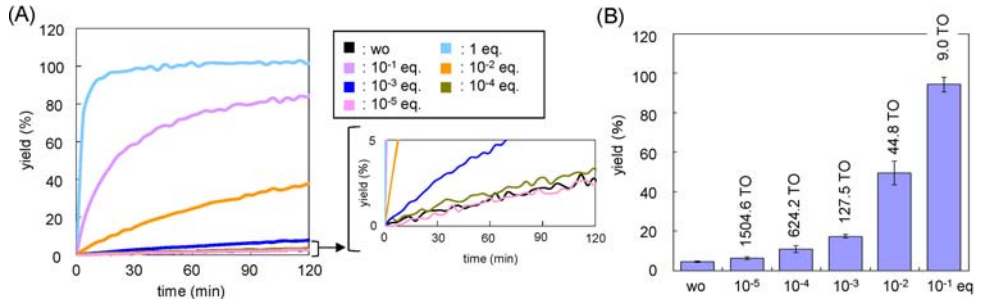

Figure 4. Turnover experiment. (A) Time course of the yield in the reaction between 50 nM CNs-AMCA and MBA probe at shown SR concentrations (50 nM to 0.5 pM) in Tris-HCl buffer (pH 7.2) containing 100 mM $MgCl_2$ at 22 °C. (B) The reaction yields after 15 h and turnover numbers (TO). The reaction yields were reported as average of values from four times.

AMCA. The inflection point of the CNs-AMCA probe was 50.0 s. In contrast to the background reactions suffered by the DNs-AMCA/MBA probe pair, however, the CNs-AMCA/MBA probe pair pleasingly provided almost no background reactions in the absence of the template, and the S/B ratio was found to be 223 after 30 s (Figure 3D).

The equilibrium constants for the formation of the double strands between the CNs-AMCA or MBA probes and the template were calculated to be 47.1×10^6 and 9.6×10^6 M^{-1}, respectively, on the basis of a thermodynamic study (Figure S4, Supporting Information). On the basis of these results, 52% of the template formed a reaction complex in the solution with the two probes binding with template at the same time at 22 °C. Although the speed of the reaction was not maximized under these experimental conditions because of the relatively low levels of the reaction complex, the apparent rate constant of the CNs-AMCA/MBA probe pair was calculated to be 2.45×10^{-2} s^{-1} (Figure S3, Supporting Information). Although an estimation of the rate constant of this chemical reaction has been provided in a later section, it is worth pointing out at this stage that the rate of this chemical reaction was much greater than that of any of the chemistries previously reported in this area of research.[1c,2b,c,3b,d,4a,5,6] For this reason, the decision was taken to use the probe pair of CNs-AMCA and MBA in the next round of turnover experiments.

For the CNs-AMCA probe to be successfully applied to the detection of a biological sample, it needs to be stable to biological compounds containing thiols, such as cysteine residues. To determine the stability of the CNs-AMCA probe, we treated the probe with different concentrations (1 μM to 1 mM) of glutathione (GSH) or dithiothreitol (DTT) and monitored the resulting fluorescence signal for 30 min (Figure S5, Supporting Information). The probe did not provide significant signal even at a 1 mM concentration of GSH or DTT. We also applied the probe to the detection of RNA in living *E. coli* cells (Figure S6, Supporting Information). Briefly, *E. coli* JM109 cells were treated with a CNs-AMCA and MBA probe pair, which targets 23S rRNA, in buffer containing a low concentration of SDS for 10 min at 25 °C, and the resulting fluorescence images were recorded using a fluorescence microscope. The CNs-AMCA and MBA matched probe pair showed strong fluorescence signals, whereas the mismatched probe pair did not provide a significant fluorescence signal. These results indicated that the probe can detect specific RNA sequences in living bacterial cells.

Turnover Measurements. We evaluated the potential for the new probe pair to provide a level of catalytic turnover that would enhance fluorescent signal amplification (Figure 1). An ideal reaction mechanism for the turnover cycle would use the DNA target as a catalyst. These conditions would typically use a large excess of the probe relative to the number of template molecules to drive the replacement of the fluorescent product with the unreacted probe. In this way, the target concentrations were varied over the range of 50 nM to 0.5 pM, and the probe concentration was held constant at a considerable excess (50 nM). Under these conditions, the fluorescence signal was continuously monitored as a function of time (Figure 4A). The turnover number was subsequently obtained by dividing the number of moles of the fluorescent product by the number of moles of the template following a reaction period of 15 h (Figure 4B). To provide a precise estimate of the actual turnover number from the templated reaction, the slight background signals were subtracted from those of identical reactions that had been conducted in the absence of a template.

To determine the optimum reaction temperature, we evaluated the effect of temperature on the turnover of the reaction using different concentrations of the DNA template (Figure S7, Supporting Information). The reaction temperature was set at 15, 22, or 37 °C. A reaction temperature of 22 °C was found to provide the best turnover number for the probe, and an additional turnover experiment was carried out at 22 °C. When the reaction was conducted with 0.1 equiv of the template (5 nM), the fluorescence signal increased rapidly and efficiently (Figure 4A), and provided a 94.2% yield of reaction product after 15 h, as calculated from the fluorescence standard (Figure 4B). In the absence of the template, a 4.5% yield of the background reaction was observed after 15 h (Figure 4B). When 0.1 equiv of the template was used, the turnover number was estimated to be 9.0 following a background signal correction. When even lower concentrations of the template were used in the range of 10^{-2} to 10^{-5} equiv, significant fluorescent signals originating from multiple turnover reactions were observed over the background signals. The experiments involving 10^{-4} (5 pM) and 10^{-5} equiv (0.5 pM) of the template indicated that the turnover numbers were 624 and 1505, respectively. To the best of our knowledge, these turnover numbers represent the highest numbers reported to date for an OTRC process. It is noteworthy that the detection limit for this process was particularly low for an OTRC-based detection system.

Steady-State Kinetic Analysis of Turnover Reaction. The current probes were designed to kinetically favor the turnover process in two different ways. First, the lengths of the probes were designed to be short, with the MBA probe existing as a 7-mer and the CNs-AMCA probe existing as an 8-mer. The shorter DNA normally provides a greater dissociation constant

dx.doi.org/10.1021/ja404743m | J. Am. Chem. Soc. 2013, 135, 14172−14178

without changing the association constant.[19] Second, the probe pairing of CNs-AMCA and MBA was designed to provide a rapid chemical reaction. It was envisaged that these properties would contribute to an efficient turnover.

Unfortunately, however, the kinetic mechanisms associated with turnover processes consisting of multiple steps remain unclear. The steady state of the turnover reaction of the OTRC has not been carefully analyzed from a kinetic perspective. With this in mind, the decision was taken in the current study to evaluate the kinetics of the turnover reaction shown in Figure 5

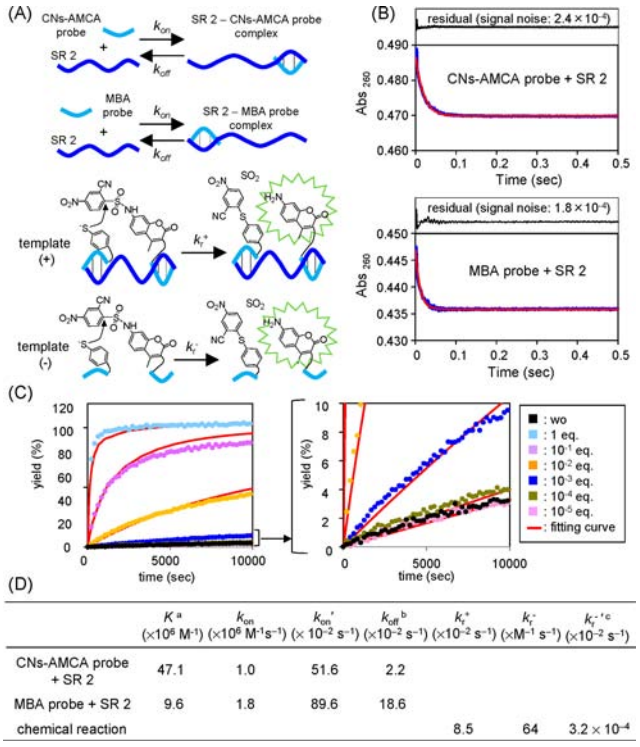

	K [a] ($\times 10^6$ M^{-1})	k_{on} ($\times 10^6$ $M^{-1}s^{-1}$)	k_{on}' ($\times 10^{-2}$ s^{-1})	k_{off} [b] ($\times 10^{-2}$ s^{-1})	k_r^+ ($\times 10^{-2}$ s^{-1})	k_r^- ($\times M^{-1}$ s^{-1})	$k_r^{-\prime}$ [c] ($\times 10^{-2}$ s^{-1})
CNs-AMCA probe + SR 2	47.1	1.0	51.6	2.2			
MBA probe + SR 2	9.6	1.8	89.6	18.6			
chemical reaction					8.5	64	3.2×10^{-4}

Figure 5. (A) Scheme of kinetic parameters. (B) Typical stopped-flow kinetics runs in this study at 22 °C, showing primary data (blue) with the best-fit single-exponential curve (red) superimposed. (C) Curve fitting analysis. Time course of the yield, showing primary data with the fitting curve (red) superimposed. The fitting was calculated by Mathematica 7 (Wolfrum). (D) Kinetic parameters for the hybridization of each probe and DNA-templated reaction. SR 2 was 21 mer ODN containing target sequence. [a]van't Hoff plot (see Figure S4, Supporting Information). [b]$k_{off} = k_{on}/K$. [c]$k_r^{-\prime} = k_r^- \times 50$ nM.

using a model scheme (see more detail in Figure S8, Supporting Information) and estimate the rate constant of the S_NAr reaction on the basis of the steady state of the turnover reaction.

We initially evaluated the association (k_{on}) and dissociation (k_{off}) rate constants from the hybridization processes of the probes and the template. Using a UV absorption spectrometer equipped with a stopped-flow, the k_{on} values for the hybridization processes of each probe were directly measured under pseudo-first-order conditions (Figure 5B). The equilibrium constants (K) of CNs-AMCA probe/SR and MBA probe/SR were also evaluated using a thermal denaturation experiment (Figure S4, Supporting Information). The k_{off} values were calculated from the K and k_{on} values by assuming normal two-state binding for the complex. The resulting kinetic parameters from the experiment, including the K, k_{on}, and k_{off} values at 22 °C, have been summarized in Figure 5D. The k_{on}' values for the probes were calculated by multiplying the corresponding k_{on} values by the concentration of the probe (CNs-AMCA or MBA), as shown in Figure 4. The association values calculated for the AMCA probe/SR and MBA probe/SR were 51.6×10^{-2} and 89.6×10^{-2} s^{-1}, respectively. These values were found to be slightly faster than the corresponding dissociation values, which were 2.2×10^{-2} and 18.6×10^{-2} s^{-1}, respectively, which allowed for the formation of the reaction complexes between the AMCA and MBA probes and the SR. It is noteworthy that a greater difference was observed between the dissociation constants than the association constants. This difference implied that the length of the probe DNA could be used to tune the dissociation constant to a much greater extent than it could be used to tune the association constant.

We then proceeded to analyze the template-concentration dependence on the OTRC using a simple scheme (Figure S8, Supporting Information) to estimate the reaction rates both in the presence and in the absence of the template (k_r^+ and k_r^-, respectively). We adopted three simple assumptions: (1) the two probes independently associate with and dissociate from the template, in that the order of the association or dissociation of a probe does not affect the association or dissociation rates of another probe to the same target; (2) the association and dissociation rates do not change before or after the fluorogenic reaction between the probes; and (3) the absorption coefficient and quantum yield values of the fluorogenic probe remain the same in the two different states of the probe, in that a template-bound probe provides the same values as a free probe. On the basis of these assumptions, we constructed a simple scheme (Figure S8, Supporting Information) and analyzed all of the data obtained from the template-concentration dependence. A global fitting was constructed for all of these data over a long time period (2.8 h) using a set of differential equations with the association and dissociation rates provided for the two probes, and estimated the rate constants of the chemical reaction both in the presence and in the absence of the template to be 8.5×10^{-2} and 64 M^{-1} s^{-1}, respectively (Figure 5C and D). To fit the experimental data, we also set a variable correlating with the value for the absorption coefficient and quantum yield of the fluorogenic probe (i.e., this constant converts the concentration of the fluorogenic probe to the fluorescence intensity). The constant was estimated to be 2.1×10^9 M^{-1} from the fitting process. This value was similar to the equivalent experimentally determined constant of 1.6×10^9 M^{-1}, supporting the validity of our estimations based on a simple model. Furthermore, the fitting curves provided an effective description of the traces obtained experimentally for the template concentrations across 5 orders of magnitude. On the basis of these results, we believe that our model has succeeded in estimating the reaction rates in the presence and in the absence of a template.

DISCUSSION

New chemistry based on the reactions between the CNs and the MBA groups offered a low detection limit of 0.5 pM, which was made possible by the efficient turnover. The turnover number is controlled by both thermodynamic and kinetic factors. The thermodynamic factors effectively maximize the theoretical turnover number without considering the total reaction time. For example, nonligation type chemistry relieves product inhibition by favoring certain thermodynamic factors, whereas ligation type chemistry provides thermodynamic drawback. The kinetic factors contribute to rate of a single turnover (Figure 1). In principle, the rate of a single turnover

dx.doi.org/10.1021/ja404743m | J. Am. Chem. Soc. 2013, 135, 14172−14178

could be increased by lowering the energy barrier of the rate limiting step to result in an increase of the turnover number over a given period of time.

Consideration of the model scheme using steady state reaction kinetics revealed the rates of turnover for the different steps of the reaction, including the association (k_{on}), chemical reaction (k_r), and dissociation (k_{off}) steps, as shown in Figure 5. The CNs/MBA reaction was rapid (k_r^+, 8.5 × 10^{-2} s^{-1}) and occurred with a very low level of background reactivity ($k_r^{-\prime}$, 3.2 × 10^{-6} s^{-1}). In contrast to other chemistries previously published in this area, which are slowest step on OTRC cycle, the rate of the CNs/MBA chemical reaction step was similar to that of dissociation step. The rate of the association (k_{on}') step was one order faster step than other two steps under the current reaction conditions (i.e., 50 nM of the probe). The rate limiting step of the turnover cycle was therefore determined to be the chemical reaction step and the dissociation step in this particular chemistry.

We then proceeded to simulate how each of the different kinetic parameters (k_{on}, k_r^+, $k_{off,}$) and the template concentration would impact on the turnover number using the model scheme (Figure S8, Supporting Information). Figure 6D shows

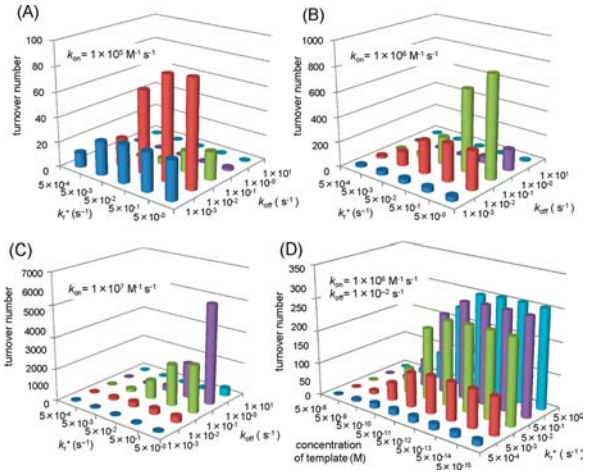

Figure 6. Simulation of turnover number. (A–C) k_r^+ versus k_{off} at 5 × 10^{-13} M template. (A) k_{on} = 1 × 10^5 M^{-1} s^{-1}, (B) k_{on} = 1 × 10^6 M^{-1} s^{-1}, (C) k_{on} = 1 × 10^7 M^{-1} s^{-1}, (D) concentration of template versus k_r^+ at k_{on} = 1 × 10^6 M^{-1} s^{-1} and k_{off} = 1 × 10^{-2} s^{-1}.

that although the turnover number increased with a reduction in the template concentration, it reached a limit at a certain concentration that was defined by k_r^+. Figure 6A,B,C indicates that an increase in the k_r^+ value together with a moderate k_{off} value maximized the turnover number. In addition, increases in the k_{on} value led to a significant increase in the turnover number. In practice, it is difficult to control the k_{on} value through the design of the nucleic acid probe. For example, although the application of a locked nucleic acid monomer enhanced the binding affinity for the complementary oligonucleotide, it is provided not from increase of k_{on} value but from decrease of k_{off} value.[13] In contrast, the k_{off} value could be readily controlled by changing the probe length. For example, the off-rate of the shorter MBA probe (7-mer) was more rapid than that of the CNs-AMCA probe (8-mer) (Figure 5D). If the target sequence is GC-rich, the probe length should be made shorter to allow for a quicker k_{off} value and the achievement of a higher turnover number. Finally, we believe there is still scope for improving the overall rapidity of the reaction through the development of new chemistry, with particular emphasis on important kinetic parameters such as k_{off} and k_r^+ toward more efficient turnovers in the nonligation type chemistry.

The CNs-AMCA/MBA probe pair was successfully applied to the detection of a specific RNA sequence in living bacterial cells. The observation of a short emission wavelength from the AMCA, however, led to an increase in the background signal derived from the biological sample. As a possible solution to this issue, it could be possible to use fluorescence dyes with longer emission wavelengths such as rhodamine or cyanine derivatives.

In conclusion, we have developed a new fluorogenic probe based on an oligonucleotide-templated S_NAr reaction. The probe completed its reaction within 30 s of being started and amplified the fluorescence signal from the very low target concentration by 1500-fold under isothermal conditions.

■ ASSOCIATED CONTENT

Supporting Information

Supporting figures, schemes, and experimental data. This material is available free of charge via the Internet at http://pubs.acs.org.

■ AUTHOR INFORMATION

Corresponding Author

h-abe@pharm.hokudai.ac.jp; y-ito@riken.jp

Notes

The authors declare no competing financial interest.

■ ACKNOWLEDGMENTS

H.A. was financially supported by the Ministry of Education, Culture, Sports, Science, and Technology (MEXT), Precursory Research for Embryonic Science and Technology (PREST) and the New Energy and Industrial Technology Development Organization (NEDO). A.S. was financially supported by a Grant-in-Aid for Young Scientists (B) (Grant No. 22790124) and the Special Postdoctoral Researcher Program of RIKEN. We are grateful for the support of BSI's Research Resources Center for mass spectra analysis.

■ REFERENCES

(1) (a) Sando, S.; Kool, E. T. *J. Am. Chem. Soc.* **2002**, *124*, 9686. (b) Abe, H.; Kool, E. T. *Proc. Natl. Acad. Sci. U. S. A.* **2006**, *103*, 263. (c) Furukawa, K.; Abe, H.; Hibino, K.; Sako, Y.; Tsuneda, S.; Ito, Y. *Bioconjugate Chem.* **2009**, *20*, 1026. (d) Pianowski, Z.; Gorska, K.; Oswald, L.; Merten, C. A.; Winssinger, N. *J. Am. Chem. Soc.* **2009**, *131*, 6492.

(2) (a) Dose, C.; Seitz, O. *Org. Lett.* **2005**, *7*, 4365. (b) Dose, C.; Ficht, S.; Seitz, O. *Angew. Chem., Int. Ed.* **2006**, *45*, 5369. (c) Dose, C.; Seitz, O. *Bioorg. Med. Chem.* **2008**, *16*, 65.

(3) (a) Ma, Z.; Taylor, J. S. *Proc. Natl. Acad. Sci. U. S. A.* **2000**, *97*, 11159. (b) Ma, Z.; Taylor, J. S. *Bioorg. Med. Chem.* **2001**, *9*, 2501. (c) Ma, Z.; Taylor, J. S. *Bioconjugate Chem* **2003**, *14*, 679. (d) Cai, J.; Li, X.; Taylor, J. S. *Org. Lett.* **2005**, *7*, 751.

(4) (a) Cai, J.; Li, X.; Yue, X.; Taylor, J. S. *J. Am. Chem. Soc.* **2004**, *126*, 16324. (b) Pianowski, Z. L.; Winssinger, N. *Chem. Commun.* **2007**, 3820. (c) Franzini, R. M.; Kool, E. T. *ChemBioChem* **2008**, *9*, 2981. (d) Abe, H.; Wang, J.; Furukawa, K.; Oki, K.; Uda, M.; Tsuneda, S.; Ito, Y. *Bioconjugate Chem.* **2008**, *19*, 1219. (e) Li, H.; Franzini, R. M.; Bruner, C.; Kool, E. T. *ChemBioChem* **2010**, *11*, 2132.

(5) (a) Grossmann, T. N.; Seitz, O. *J. Am. Chem. Soc.* **2006**, *128*, 15596. (b) Grossmann, T. N.; Seitz, O. *Chem.—Eur. J.* **2009**, *15*, 6723.

(6) Sando, S.; Sasaki, T.; Kanatani, K.; Aoyama, Y. *J. Am. Chem. Soc.* **2003**, *125*, 15720.
(7) (a) Silverman, A. P.; Kool, E. T. *Chem. Rev.* **2006**, *106*, 3775. (b) Silverman, A. P.; Kool, E. T. *Adv. Clin. Chem.* **2007**, *43*, 79.
(8) Franzini, R. M.; Kool, E. T. *Org. Lett.* **2008**, *10*, 2935.
(9) (a) Okamoto, A.; Tanabe, K.; Inasaki, T.; Saito, I. *Angew. Chem., Int. Ed.* **2003**, *42*, 2502. (b) Tanabe, K.; Nakata, H.; Mukai, S.; Nishimoto, S. I. *Org. Biomol. Chem.* **2005**, *3*, 3893. (c) Röthlingshöfer, M.; Gorska, K.; Winssinger, N. *J. Am. Chem. Soc.* **2011**, *133*, 18110.
(10) (a) Arian, D.; Cló, E.; Gothelf, K. V.; Mokhir, A. *Chem.—Eur. J.* **2010**, *16*, 288. (b) Arian, D.; Kovbasyuk, L.; Mokhir, A. *Inorg. Chem.* **2011**, *50*, 12010. (c) Röthlingshöfer, M.; Gorska, K.; Winssinger, N. *Org. Lett.* **2011**, *14*, 482. (d) Sadhu, K. K.; Winssinger, N. *Chem.—Eur. J.* **2013**, *19*, 8182.
(11) (a) Prusty, D. K.; Herrmann, A. *J. Am. Chem. Soc.* **2010**, *132*, 12197. (b) Prusty, D. K.; Kwak, M.; Wildeman, J.; Herrmann, A. *Angew. Chem., Int. Ed.* **2012**, *51*, 11894.
(12) Grossmann, T. N.; Strohbach, A.; Seitz, O. *ChemBioChem* **2008**, *9*, 2185.
(13) Christensen, U.; Jacobsen, N.; Rajwanshi, V. K.; Wengel, J.; Koch, T. *Biochem. J.* **2001**, *354*, 481.
(14) Shibata, A.; Abe, H.; Ito, M.; Kondo, Y.; Shimizu, S.; Aikawa, K.; Ito, Y. *Chem. Commun.* **2009**, 6586.
(15) Crich, D.; Sharma, I. *Angew. Chem., Int. Ed.* **2009**, *48*, 7591.
(16) Fuchs, B. M.; Syutsubo, K.; Ludwig, W.; Amann, R. *Appl. Environ. Microbiol.* **2001**, *67*, 961.
(17) Jaffe, E. K.; Cohn, M. *Biochemistry* **1978**, *17*, 652.
(18) Gough, J. D.; Gargano, J. M.; Donofrio, A. E.; Lees, W. J. *Biochemistry* **2003**, *42*, 11787.
(19) Koval, V. V.; Gnedenko, O. V.; Ivanov, Y. D.; Fedorova, O. S.; Archakov, A. I.; Knorre, D. G. *IUBMB Life* **1999**, *48*, 317.